AEM
Journals.ASM.org

Two Phages, phiIPLA-RODI and phiIPLA-C1C, Lyse Mono- and Dual-Species Staphylococcal Biofilms

Diana Gutiérrez,[a] Dieter Vandenheuvel,[b] Beatriz Martínez,[a] Ana Rodríguez,[a] Rob Lavigne,[b] Pilar García[a]

Instituto de Productos Lácteos de Asturias (IPLA-CSIC), Departamento de Tecnología y Biotecnología de Productos Lácteos Villaviciosa, Asturias, Spain[a]; Laboratory of Gene Technology, KU Leuven, Leuven, Belgium[b]

Phage therapy is a promising option for fighting against staphylococcal infections. Two lytic phages, vB_SauM_phiIPLA-RODI (phiIPLA-RODI) and vB_SepM_phiIPLA-C1C (phiIPLA-C1C), belonging to the *Myoviridae* family and exhibiting wide host ranges, were characterized in this study. The complete genome sequences comprised 142,348 bp and 140,961 bp and contained 213 and 203 open reading frames, respectively. The gene organization was typical of *Spounavirinae* members, with long direct terminal repeats (LTRs), genes grouped into modules not clearly separated from each other, and several group I introns. In addition, four genes encoding tRNAs were identified in phiIPLA-RODI. Comparative DNA sequence analysis showed high similarities with two phages, GH15 and 676Z, belonging to the *Twort-like virus* genus (nucleotide identities of >84%); for phiIPLA-C1C, a high similarity with phage phiIBB-SEP1 was observed (identity of 80%). Challenge assays of phages phiIPLA-RODI and phiIPLA-C1C against planktonic staphylococcal cells confirmed their lytic ability, as they were able to remove 5 log units in 8 h. Exposure of biofilms to phages phiIPLA-RODI and phiIPLA-C1C reduced the amount of adhered bacteria to about 2 log units in both monospecies and dual-species biofilms, but phiIPLA-RODI turned out to be as effective as the mixture of both phages. Moreover, the frequencies of bacteriophage-insensitive mutants (BIMs) of *Staphylococcus aureus* and *S. epidermidis* with resistance to phiIPLA-RODI and phiIPLA-C1C were low, at $4.05 \times 10^{-7} \pm 2.34 \times 10^{-9}$ and $1.1 \times 10^{-7} \pm 2.08 \times 10^{-9}$, respectively. Overall, a generally reduced fitness in the absence of phages was observed for BIMs, which showed a restored phage-sensitive phenotype in a few generations. These results confirm that lytic bacteriophages can be efficient biofilm-disrupting agents, supporting their potential as antimicrobials against staphylococcal infections.

Two staphylococcal species, *Staphylococcus aureus* and *Staphylococcus epidermidis*, are the main causes of nosocomial infections due to their ability to adhere to, colonize, and develop biofilms in medical devices and human organs (1). Staphylococcal biofilms are complex structures in which bacterial cells are surrounded by an extracellular material (polysaccharides, teichoic acids, proteins, and extracellular DNA) which confers protection against antibacterial drugs and the host immune system. In addition, growth of bacteria in a biofilm facilitates the development of antibiotic-resistant organisms (2). *S. epidermidis* is one of the most abundant species in the human skin microbiota, from which it easily reaches catheters, heart valves, and contact lenses. Despite being regarded as an innocuous bacterium, it is now accepted as an opportunistic pathogen and one of the most common causes of bacteremia in immunocompromised patients (3), preterm infants (4), and biofilm-related infections (5). In addition, resistance to methicillin due to the presence of the *mecA* gene is widely spread in hospital isolates (6). Similarly, virulence in *S. aureus* is mainly due to its ability to adhere to and proliferate on biotic and abiotic surfaces (7). In hospital settings, *S. aureus* infections affecting internal organs and implanted medical devices have become difficult to eradicate. Moreover, methicillin-resistant *S. aureus* (MRSA) strains are often prevalent in hospitals and have recently spread to nonrelated environments, affecting people without exposure to the health care environment (8). MRSA strains have also been isolated from foods of animal origin (9) and from livestock (10).

Phage therapy exploits the ability of phages to infect and kill bacteria in the treatment of infectious diseases. This represents a potential alternative to antibiotics to fight against multiresistant pathogenic bacteria or superbugs (11). Indeed, human trials with phages against a number of infections have confirmed their safety and shown that phage therapy can provide good results for untreatable chronic infections (12, 13). Specifically, recent results showed the efficacy of phages in animal models, such as *S. aureus* septicemia in mice (14) and in silkworms (15). The safety and efficacy of phage products for removal of this bacterium in a sinusitis sheep model have also been proven (16). Other applications of phages against *S. aureus* encompass improvements in wound healing developed on diabetic patients (17, 18) and the treatment of chronic wounds (19). Previous results also showed the ability of phages to remove biofilms formed by staphylococcal species (20–22).

In this study, we report a complete morphological and genetic characterization of two new phages infecting staphylococcal species, named vB_SauM_phiIPLA-RODI (phiIPLA-RODI) and vB_SepM_phiIPLA-C1C (phiIPLA-C1C) following the nomenclature proposed by Kropinski et al. (23). The lytic abilities of these phages, including host range and biofilm removal, were analyzed. Furthermore, the

Received 28 October 2014 **Accepted** 27 February 2015

Accepted manuscript posted online 6 March 2015

Citation Gutiérrez D, Vandenheuvel D, Martínez B, Rodríguez A, Lavigne R, García P. 2015. Two phages, phiIPLA-RODI and phiIPLA-C1C, lyse mono- and dual-species staphylococcal biofilms. Appl Environ Microbiol 81:3336–3348. doi:10.1128/AEM.03560-14.

Editor: K. E. Wommack

Address correspondence to Pilar García, pgarcia@ipla.csic.es.

Supplemental material for this article may be found at http://dx.doi.org/10.1128/AEM.03560-14.

doi:10.1128/AEM.03560-14

TABLE 1 Strains used in this study, with origins and phage sensitivities, expressed as efficiencies of plaque formation (EOP)

Species	Strain	Origin	Reference	EOP[a]	
				phiIPLA-RODI	phiIPLA-C1C
S. aureus	IPLA-1	Dairy industry surfaces	66	1	—
	IPLA-2	Dairy industry surfaces	66	0.98 ± 0.03	—
	IPLA-3	Dairy industry surfaces	66	0.87 ± 0.06	—
	IPLA-4	Dairy industry surfaces	66	1.03 ± 0.04	—
	IPLA-5	Dairy industry surfaces	66	0.91 ± 0.01	—
	IPLA-6	Meat industry surfaces	66	1.01 ± 0.03	—
	IPLA-7	Meat industry surfaces	66	0.99 ± 0.03	—
	IPLA-8	Meat industry surfaces	66	0.85 ± 0.11	—
	IPLA-9	Meat industry surfaces	66	0.92 ± 0.23	—
	IPLA-10	Meat industry surfaces	66	0.87 ± 0.07	—
	IPLA-11	Meat industry surfaces	66	0.89 ± 0.06	0.09 ± 0.01
	IPLA-12	Meat industry surfaces	66	0.79 ± 0.05	—
	IPLA-13	Meat industry surfaces	66	1.02 ± 0.03	—
	IPLA-14	Meat industry surfaces	66	0.96 ± 0.02	—
	IPLA-15	Meat industry surfaces	66	1.02 ± 0.03	—
	IPLA-16	Meat industry surfaces	66	1.23 ± 0.04	1.09 ± 0.07
	IPLA-17	Meat industry surfaces	66	1.06 ± 0.01	—
	IPLA-18	Meat industry surfaces	66	0.96 ± 0.02	0.39 ± 0.05
	IPLA-19	Milk sample	Unpublished data	1.12 ± 0.03	—
	15981	Clinical isolate	67	0.99 ± 0.02	—
	V329	Bovine subclinical mastitis	68	1.01 ± 0.01	—
S. epidermidis	F12	Women's breast milk	69	—	1
	B	Women's breast milk	69	0.19 ± 0.01	0.78 ± 0.01
	DH3LIK	Women's breast milk	69	—	0.56 ± 0.07
	YLIC13	Women's breast milk	69	—	0.77 ± 0.06
	Z2LDC14	Women's breast milk	69	—	0.62 ± 0.03
	DG2ñ	Women's breast milk	69	—	0.88 ± 0.06
	ASLD1	Women's breast milk	69	—	0.62 ± 0.04
	LO5081	Women's breast milk	69	0.87 ± 0.04	1.23 ± 0.04
	LX5RB4	Women's breast milk	69	—	0.89 ± 0.02
	LO5RB1	Women's breast milk	69	—	0.97 ± 0.03
Staphylococcus haemolyticus	ZL89-3	Women's breast milk	70	0.91 ± 0.03	—
	ZL114-1	Women's breast milk	70	0.87 ± 0.02	—
Staphylococcus hominis	ZL31-13	Women's breast milk	70	0.77 ± 0.05	—
	ZL5-5	Women's breast milk	70	0.68 ± 0.01	—
Staphylococcus arlettae	ZL114-5	Women's breast milk	70	0.45 ± 0.03	—
	ZL98-5	Women's breast milk	70	0.55 ± 0.08	0.23 ± 0.04
Staphylococcus lugdunensis	ZL5-11	Women's breast milk	70	0.69 ± 0.04	0.56 ± 0.05
Staphylococcus gallinarum	ZL90-5	Women's breast milk	70	0.71 ± 0.06	0.68 ± 0.01
Staphylococcus kloosii	ZL74-2	Women's breast milk	70	0.46 ± 0.03	0.65 ± 0.01
Staphylococcus pasteuri	ZL16-6	Women's breast milk	70	0.45 ± 0.06	—
Staphylococcus xylosus	ZL61-2	Women's breast milk	70	0.65 ± 0.02	0.56 ± 0.01
Staphylococcus saprophyticus	ZL112-15	Women's breast milk	70	0.89 ± 0.08	0.37 ± 0.04
Staphylococcus sciuri	IPLA301	Women's breast milk	70	0.98 ± 0.05	—
Macrococcus caseolyticus	IPLA101	Dairy industry surface	Unpublished data	0.65 ± 0.03	0.06 ± 0.03

[a] Data are means ± standard deviations calculated for three independent experiments. —, resistance to the phage.

frequency of bacteriophage-insensitive mutants (BIMs) of planktonic cells was calculated for both phages, and a preliminary characterization of these resistant bacteria is also presented.

MATERIALS AND METHODS

Bacterial strains, bacteriophages, and growth conditions. Forty-four different staphylococcal species and one *Macrococcus caseolyticus* strain were used in this study (Table 1). All the bacteria were isolated in Baird-Parker (BP) agar and were routinely cultured in tryptic soy broth (TSB; Scharlau, Barcelona, Spain) at 37°C with shaking or on TSB plates containing 2% (wt/vol) bacteriological agar (TSA).

To select *S. aureus* IPLA16 colonies resistant to rifampin (*S. aureus* IPLA16-rif^R), 100-μl aliquots of overnight cultures were plated onto TSA plates supplemented with 100 μg/ml of rifampin. Plates were incubated for 16 h at 37°C. Single colonies were picked up and grown in fresh TSB at 37°C with shaking for further studies.

Bacteriophages phiIPLA-RODI and phiIPLA-C1C were propagated on *S. aureus* IPLA1 and *S. epidermidis* F12, respectively, as previously described (24).

Bacteriophage isolation and propagation. Bacteriophages were isolated from a sewage treatment plant in Colunga, Asturias, Spain. For isolation of staphylococcal phages, 1 liter of sewage was centrifuged twice at 13,600 × *g* for 30 min, and the supernatant was filtered using 0.45-μm and 0.22-μm cellulose acetate membrane filters sequentially (VWR, Spain). Enrichment cultures were performed by mixing 20 ml of TSB concentrated five times (5× TSB), 80 ml of filtered sewage, and 100 μl of overnight culture from one of four mixtures of *S. aureus* strains (mixture 1, *S. aureus* IPLA3, IPLA4, IPLA6, IPLA15, IPLA16, IPLA17, and IPLA18; mixture 2, *S. aureus* IPLA5, IPLA8, and IPLA14; mixture 3, *S. aureus* IPLA1, IPLA2, IPLA9, and IPLA10; and mixture 4, *S. aureus* IPLA7 and IPLA13). After incubation for 16 h at 37°C, the samples were centrifuged and filtered. A total of three enrichments were carried out to obtain higher phage titrations. To assess the presence of phages, 5-μl aliquots of the supernatants from the different combinations were spotted onto bacterial lawns of each of the *S. aureus* and *S. epidermidis* strains following the double-layer technique (24). The presence of an inhibition halo was considered representative of phage sensitivity. Each inhibition halo was further purified to isolate different phages. Two phages were reisolated, propagated, and purified by use of a CsCl continuous-density gradient as described previously (24). As host bacteria, *S. aureus* IPLA1 and *S. epidermidis* F12 were used for the propagation and purification of phages phiIPLA-RODI and phiIPLA-C1C, respectively.

Bacteriophage one-step growth curves, EOP, and stabilities at various pHs and temperatures. One-step growth curves were performed with phages phiIPLA-RODI and phiIPLA-C1C, using the sensitive strains *S. aureus* IPLA16 and *S. epidermidis* LO5081, respectively, as previously described (24). Bacteriophage host ranges were determined using phiIPLA-RODI (10^9 PFU/ml) and phiIPLA-C1C (10^9 PFU/ml) in the drop test, and titrations of the phages were further carried out with all sensitive strains to differentiate between infection and lysis due to bacteriocins. The efficiency of plaque formation (EOP) was determined by dividing the phage titer on the test strain by the phage titer on the reference strain (*S. aureus* IPLA1 for phage phiIPLA-RODI and *S. epidermidis* F12 for phage phiIPLA-C1C).

The pH stability of the phage particles was tested by incubation in Britton-Robinson pH universal buffer (150 mM KCl, 10 mM KH_2PO_4, 10 mM sodium citrate, 10 mM H_3BO_3, with adjustment of the pH in the range from 3 to 11) for 3 h at room temperature. Similarly, the temperature stability was examined by incubating the phages in SM buffer (20 mg/liter Tris-HCl, 10 mg/liter $MgSO_4$, 10 mg/liter $CaCl_2$, 100 mg/liter NaCl, pH 7.5) at different temperatures (ranging from 40°C to 90°C) for 30 min. Phage suspensions in SM buffer at 4°C were used as controls.

Bacterium-phage challenge test with planktonic staphylococcal cultures. Ten milliliters of TSB broth was inoculated with an overnight culture to an optical density at 600 nm (OD_{600}) of 0.05 and then incubated at 37°C with shaking until reaching an OD_{600} of 0.1 (10^7 CFU/ml). A 100-fold dilution of the culture was infected at a multiplicity of infection (MOI) of 100 (10^7 PFU/ml). Infected cultures were incubated for 8 h at 37°C, and samples were taken at 2-h intervals. Phage and cell counts were performed in triplicate.

Biofilm formation and biofilm-phage challenge test. Overnight cultures of *S. aureus* IPLA16-rif^R and *S. epidermidis* LO5081 were diluted to 10^6 CFU/ml in fresh TSB supplemented with 0.25% glucose. Aliquots of 200 μl of each single culture or mixture of both strains (100 μl of each strain) were poured into a 96-microwell plate (Thermo Scientific, Madrid, Spain). Biofilms were grown for 24 h at 37°C. Wells were then washed twice with PBS (137 mM NaCl, 2.7 mM KCl, 10 mM Na_2HPO_4, and 2 mM KH_2PO_4; pH 7.4). To test biofilm degradation by each phage, 100 μl of SM buffer and 100 μl of phiIPLA-RODI or phiIPLA-C1C were added to each well (10^9 PFU/well). To test the combined effect of both phages, 200 μl of the mixture of both phages was added to the well (10^9 PFU/well of each phage). SM buffer was added for control purposes. The plates were incubated for 4 h at 37°C, the supernatants were removed, and serial dilutions were plated on TSA plates. The cells that were still bound after phage treatment were collected by scratching twice with a sterile swab, suspended in 9 ml of SM buffer, and vigorously vortexed for 1 min. Serial dilutions were plated for bacterial counting. For mixed biofilms, *S. epidermidis* counts were calculated as the differences between total staphylococcal counts in TSA and the *S. aureus* IPLA16-rif^R counts in TSA supplemented with 100 μg/ml of rifampin.

Alternatively, the biomass adhered to the well was observed by staining with crystal violet (0.1% [wt/vol]) as described previously (25).

Isolation and characterization of BIMs. Bacteriophage-insensitive mutants (BIMs) resistant to phages phiIPLA-RODI and phiIPLA-C1C were obtained from strains *S. aureus* IPLA16 and *S. epidermidis* LO5081, respectively. Aliquots of 100 μl of overnight culture of each strain (10^8 CFU) were incubated with 100 μl of phage (10^9 PFU) for 10 min at 37°C. The mixture was then poured onto a 2% TSA plate and covered with 3 ml of 0.7% TSA. Plates were incubated for 16 h at 37°C. Surviving colonies were picked up and grown in fresh TSB medium for 16 h at 37°C. Bacteriophage susceptibility was tested by the drop assay (24). The BIM frequency was calculated as the ratio between the number of surviving colonies and the initial number of bacteria incubated in the presence of phage.

Surface hydrophobicity was determined according to the microbial adhesion to solvents (MATS) assay, using hexadecane (Sigma-Aldrich, Madrid, Spain) and stationary-phase cells washed with 0.15 M NaCl and adjusted to a final OD_{600} of 0.8 (26). Each measurement was performed in triplicate, and the assay was carried out twice with independent cultures.

The susceptibilities of *S. aureus* IPLA16, *S. epidermidis* LO5081, and their respective BIMs to several NaCl concentrations were evaluated by determining the 50% lethal dose (LD_{50}) values, defined as the concentration of NaCl that inhibited the growth of the strain by 50% compared with the control culture of the same strain growing in standard TSB (0.5% NaCl). Overnight cultures were diluted to an OD_{600} of 0.05 in TSB containing different NaCl concentrations (0.5 to 20%). Aliquots of 0.2 ml were placed into 96-microwell plates (Nunclon D surface; Nunc, Roskilde, Denmark). Plates were incubated at 37°C, and growth was monitored in a Benchmark Plus microplate spectrophotometer (Bio-Rad Laboratories) until the control samples reached an OD_{600} of 0.9 ± 0.1. Growth rates were estimated by linear regression after plotting the $\ln(OD_{600})$ as a function of time during the exponential growth phase, as described previously (27). The adsorption kinetics and the adsorption rate constants (k) of the phages were calculated as previously described (28).

Electron microscopy of phage particles. Electron microscopic examination was performed after negative staining of the phage particles with 2% uranyl acetate. Electron micrographs were taken using a JEOL 12.000 EXII transmission electron microscope (JEOL USA Inc., Peabody, MA).

DNA extraction and protein analysis. To prepare bacterial DNA-free samples for sequence analysis, the purified phages were treated as described previously (20). Analysis of virion proteins was carried out by SDS-PAGE analysis and matrix-assisted laser desorption ionization–tandem time of flight (MALDI-TOF/TOF) mass spectrometry as previously described (29).

Bacteriophage genome analysis and characterization. The genome sequences of phages phiIPLA-RODI and phiIPLA-C1C were determined by GenProbio SRL (Parma, Italy), using an Ion Torrent personal genome machine (PGM; Life Technologies). The MIRA program (version 3.4.0) was used for assembly of genome sequences, resulting in 138-fold coverage for phiIPLA-C1C and 432-fold coverage for phiIPLA-RODI. Additional sequencing using specific primers was done to elucidate regions with ambiguities. Phage genomes were autoannotated using RAST (30) and were manually curated. BLASTX and BLASTP were used to search for similar proteins (31). Structural predictions and motif searches were performed with InterProScan (32). Putative promoters and Shine-Dalgarno sites were predicted using the software MEME (33) followed by visual inspection. ARNold (34) and TransTerm (35) were used to detect poten-

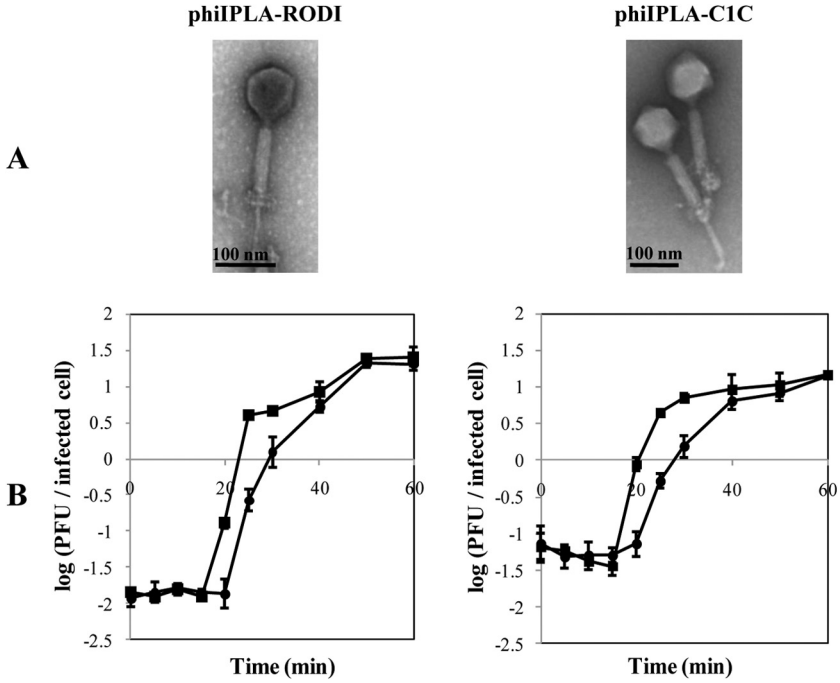

FIG 1 (A) Transmission electron microphotographs of phages phiIPLA-RODI and phiIPLA-C1C. (B) One-step growth curves of phage phiIPLA-RODI in *S. aureus* IPLA16 and phage phiIPLA-C1C in *S. epidermidis* LO5081. Values correspond to the numbers of PFU per infected cell in chloroform-treated cultures (■) and untreated cultures (●). Each data point shows the mean ± standard deviation for three independent experiments.

tial rho-independent terminators. Putative tRNAs were predicted using tRNAscan-SE (36) and ARAGORN (37). Genomic comparison at the nucleotide level was made with EMBOSS Stretcher (38) and with MAUVE (39), using the genome sequences available in public databases (July 2014) for phages of the *Myoviridae* family infecting *Staphylococcus*. Before the global alignments could be performed, the genomes were manually colinearized, placing the arbitrary starting point at the end of the open reading frame (ORF) preceding the large terminase subunit gene. The genome organization of the phages and comparative BLASTN figures were generated using CGView server (40). Annotation was done on the basis of homology with previously described phages.

Statistical analysis. Statistical analyses were performed to establish any significant differences between the control and tested strains. The differences are expressed as means ± standard deviations for three biological replicates for all assays and were determined by one-way analysis of variance (ANOVA) followed by the Bonferroni multicomparison test. *P* values of <0.05 were considered statistically significant.

Nucleotide sequence accession numbers. The sequences of phiIPLA-RODI and phiIPLA-C1C have been deposited in GenBank under accession numbers KP027446 and KP027447, respectively.

RESULTS

Bacteriophages phiIPLA-RODI and phiIPLA-C1C, two new members of the *Myoviridae* family that infect staphylococcal species. Two phages were isolated from sewage after enrichment with four different mixtures of *S. aureus* strains. From mixtures 1 and 4, two phages were further isolated, propagated, and purified, using *S. aureus* IPLA1 as the host for phage phiIPLA-RODI and *S. epidermidis* F12 for phage phiIPLA-C1C. The host ranges of the isolated bacteriophages were determined by testing against a collection of 47 bacterial strains (Table 1). Both phages showed a wide host range, infecting 81% (phiIPLA-RODI) and 40% (phiIPLA-C1C) of the *Staphylococcus* strains tested. For *S. aureus*, all strains were infected by phiIPLA-RODI, whereas phiIPLA-C1C infected only three strains. All *S. epidermidis* strains were infected by phiIPLA-C1C, indicating that phage phiIPLA-C1C is more specific for *S. epidermidis*. In addition, 10 different species belonging to the *Staphylococcus* genus were also sensitive to phiIPLA-RODI, and 6 of them were sensitive to phiIPLA-C1C. Both phages were able to infect the *Macrococcus caseolyticus* IPLA101 strain (Table 1).

Virions of both phages were observed by transmission electron microscopy, and they showed isometric capsids and long contractile tails typical of the *Myoviridae* family (Fig. 1A). phiIPLA-RODI has a capsid of 73 ± 8 nm in diameter and a tail that is 95 ± 8 nm long. phiIPLA-C1C has a capsid of 88 ± 10 nm in diameter and a tail that is 110 ± 13 nm long. A double baseplate upon tail contraction, which is typical of SPO1-related phages, was clearly observed in both phages (41).

One-step growth curves under standardized conditions were determined for both phages (Fig. 1B). The eclipse and latent periods of phiIPLA-RODI on *S. aureus* IPLA16 and of phiIPLA-C1C on *S. epidermidis* LO5081 were 15 and 20 min, respectively. The burst sizes were estimated to be 25 and 15 phage particles per infected cell for phiIPLA-RODI and phiIPLA-C1C, respectively (Fig. 1B).

Both phages appeared to be quite stable at temperatures below 60°C, but a total inactivation of the phages at temperatures over 70°C was observed (see Fig. S1 in the supplemental material). Concerning pH stability, a notable reduction of 3.6 log units in the phage titer was observed for phage phiIPLA-C1C at pH 11, while phiIPLA-RODI was found to be quite stable at this pH. No viable phages were recovered after incubation at pH 3 (see Fig. S1).

The genomic organization of phages phiIPLA-RODI and phiIPLA-C1C is typical of the *Spounaviridae* subfamily. The ge-

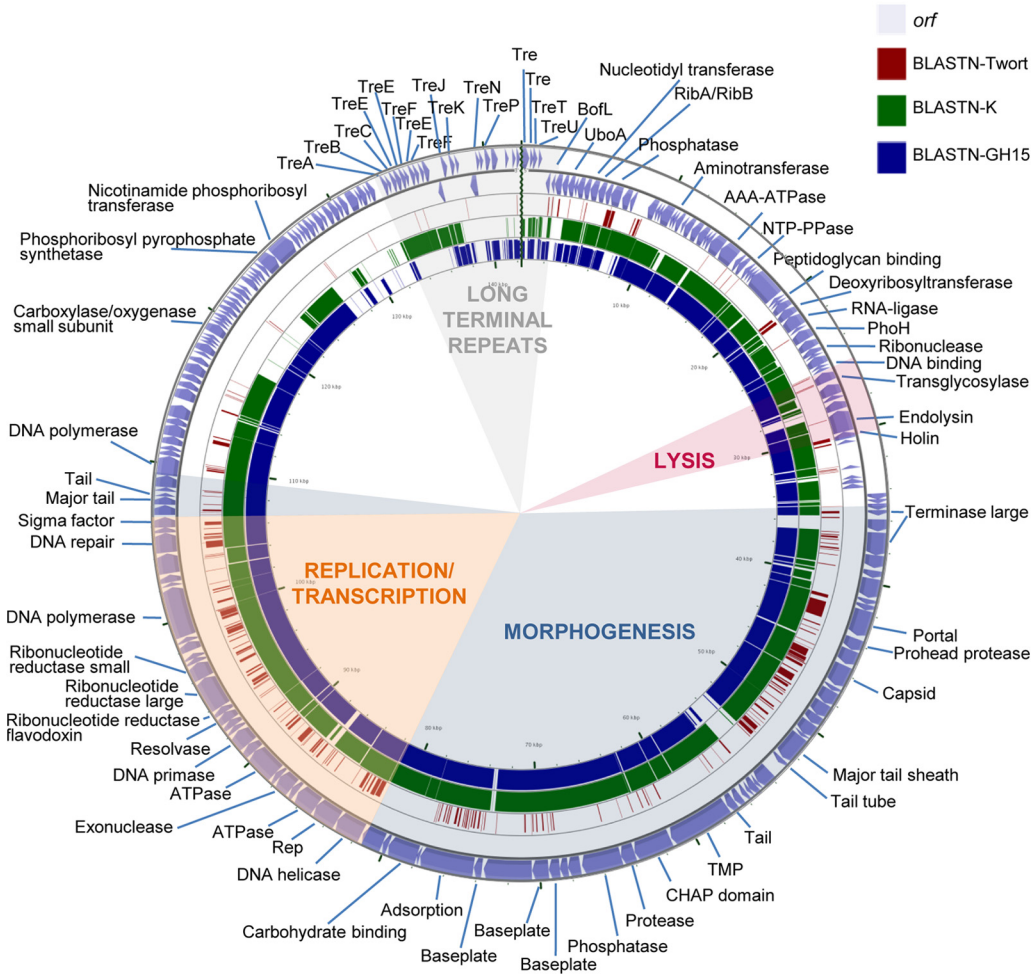

FIG 2 Genome organization of phage phiIPLA-RODI and BLASTN comparisons. The outer ring with arrows represents the ORFs of the circularized phage. The predicted gene functions are also indicated. The different functional modules in the genome are shown by colored shading. BLASTn analysis, whose results are represented by each inner ring, was performed with the representative phages Twort (dark red), K (green), and (most similar) GH15 (blue).

nomes of phiIPLA-RODI and phiIPLA-C1C are double-stranded linear DNA molecules of 142,348 bp (carrying 213 putative ORFs) and 140,961 bp (carrying 203 putative ORFs), respectively, with ORFs preceded by potential Shine-Dalgarno sequences (see Tables S1 and S2 in the supplemental material). Up to 40 and 27 putative promoters (see Table S3), respectively, were identified, and most of them showed AT-rich sequences upstream of the −35 region and corresponded to middle or early promoters. In addition, 52 and 33 putative rho-independent terminators were predicted for phiIPLA-RODI and phiIPLA-C1C, respectively (Table S4). Two main transcriptional units were identified in both phages (Fig. 2 and 3).

Based on BLAST analysis and conserved domain screening, putative functions have been assigned to 93 of the predicted ORFs (44%) from phiIPLA-RODI and 80 of the predicted ORFs (39%) from phiIPLA-C1C (see Tables S1 and S2, respectively). ORFs were annotated based on the similarities of phiIPLA-RODI and phiIPLA-C1C to phage K (accession number NC_005880) and *S. epidermidis* phage phiIBB-SEP1 (accession number KF021268.1), respectively.

Overall, genes of both phages are organized into four functional modules, including genes for long terminal repeats (LTRs), morphogenesis, cell lysis, and replication/transcription. Furthermore, the phiIPLA-RODI genome carries a tRNA gene between *orf18* and *orf19*, encoding $tRNA_{Met}$, and three tRNA genes between *orf59* and *orf60*, encoding $tRNA_{Asp}$, $tRNA_{Phe}$, and $tRNA_{Trp}$. The presence of a conserved sequence (TGTCAAGTTAATTT) was detected near these tRNA genes, at positions 8852 to 8865, 31999 to 32012, and 32179 to 32192, which may be binding sites for a transcriptional regulatory factor (42). No tRNA genes were identified in the phiIPLA-C1C genome.

The ends of the genomes of both phages are flanked by LTRs, which are putatively involved in the recombination of phage genomes inside the cell. These regions encode small proteins implicated in host takeover, redirecting cell metabolism to phage production (43). The exact boundaries between these LTRs and the rest of the genome have not been determined, but comparison with the terminal repeat proteins of other phages suggests that they may span from the TreA (*orf192*)- to the BofL (*orf6*)-encoding genes in phiIPLA-RODI. In this fragment, genes encoding 28 putative terminal repeat proteins were detected. In addition to the previously described TreA protein gene, the homologous TreB,

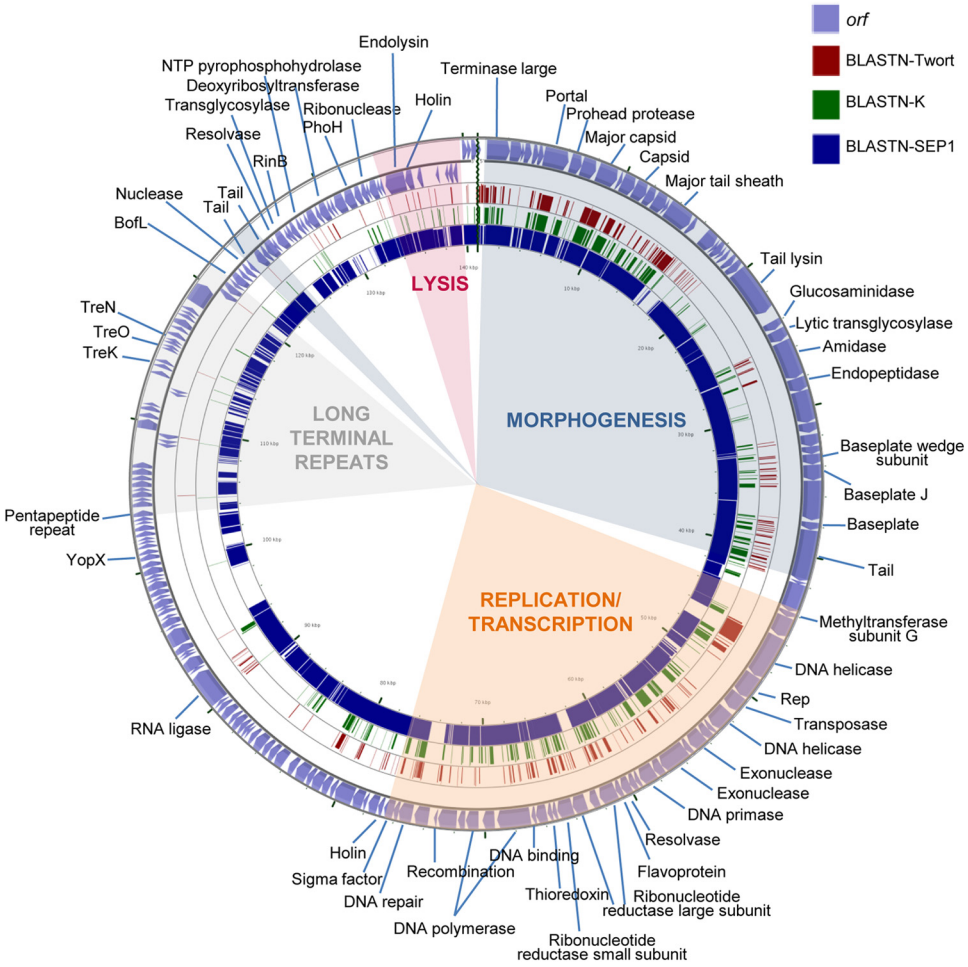

FIG 3 Genome organization of phage phiIPLA-C1C and BLASTN comparisons. The outer ring with arrows represents the ORFs of the circularized phage. The predicted gene functions are indicated. The different functional modules in the genome are shown by colored shading. BLASTn analysis, whose results are represented by each inner ring, was performed with the representative phages Twort (dark red), K (green), and (most similar) phiIBB-SEP1 (blue).

TreC, TreE, TreF, TreJ, TreK, TreN, TreP, TreU, and TreT protein genes were recognized in a region of 10,330 bp. In addition, the gene for a putative group I homing HNH endonuclease (*orf206*), which is typical of this region, was also identified. In phiIPLA-C1C, LTRs could be expanded from the pentapeptide repeat protein gene (*orf143*) to the BofL gene (*orf165*), with a total of 11,844 bp and genes encoding 23 putative proteins. In this region, genes for three putative terminal repeat proteins, with homology to TreK (*orf150*), TreO (*orf152*), and TreN (*orf155*), were identified.

The morphogenesis module was split into two regions in both genomes. In phiIPLA-RODI, these regions (*orf67* to *orf108* and *orf135* to *orf139*) were separated by the replication/transcription module, whereas the LTR region and the replication/transcription module were located between the two morphogenetic regions (*orf1* to *orf42* and *orf169* to *orf171*) in phiIPLA-C1C. Genes encoding the large terminase subunit, portal protein, prohead protease, major capsid, major tail sheath, and tape measure protein (TMP) were identified. The large terminase subunit of phiIPLA-RODI (*orf67*) presented a group I intron interspaced in the gene, while this intron was not present in phiIPLA-C1C (*orf2*). The remainder of the proteins encoded in these regions failed to show similarity to the terminase small subunits. The TMP-encoding gene is followed by two putative genes in phiIPLA-RODI: *orf95*, which encodes a tail-associated protein with muralytic activity (as deduced from the presence of a CHAP domain); and *orf96*, which encodes a protein with a predicted endopeptidase domain. Moreover, the product of *orf97* showed homology with glycerol-phosphodiester hydrolytic activities. In phiIPLA-C1C, the TMP-encoding gene is followed by four putative genes: *orf28*, encoding a glucosaminidase; *orf29*, encoding a lytic transglycosylase; *orf30*, encoding an amidase with a CHAP domain; and *orf31*, encoding a peptidase. The other genes in these modules are likely to encode baseplate, structural, and assembly proteins. Protein analysis of viral particles allowed the identification of the adsorption-associated tail protein (*orf104*), major tail sheath protein (*orf85*), capsid protein (*orf78*), and major tail protein (*orf136*) in phage phiIPLA-RODI. In phage phiIPLA-C1C, a tail protein (*orf40*), major tail sheath (*orf18*), major capsid protein (*orf11*), and a hypothetical protein (*orf85*) were also identified (Fig. 4).

The lysis modules, containing genes involved in bacterial lysis (holin and endolysin), were located upstream of the morphogenetic module. In addition, putative transglycosylase-encoding genes (*orf53* in phiIPLA-RODI and *orf174* in phiIPLA-C1C),

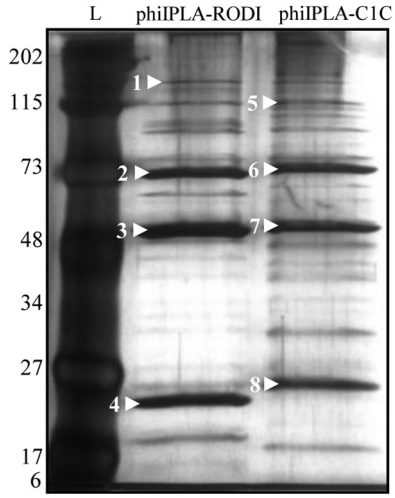

FIG 4 Analysis by SDS-PAGE and silver staining of the structural proteins of phages phiIPLA-RODI and phiIPLA-C1C. Protein molecular size markers (kDa) are shown on the left (lane L). Bands marked with white arrowheads were identified by mass spectrophotometry. The proteins in phage phiIPLA-RODI were the adsorption-associated tail protein (*orf104*) (1), the major tail sheath protein (*orf85*) (2), the capsid protein (*orf78*) (3), and the major tail protein (*orf136*) (4). The proteins in phage phiIPLA-C1C were the tail protein (*orf40*) (5), the major tail sheath (*orf18*) (6), the major capsid protein (*orf11*) (7), and a hypothetical protein (*orf85*) (8).

which may be involved in cell wall hydrolysis, were also identified. Moreover, in phiIPLA-C1C, a second holin gene (*orf78*) was located downstream of the replication/transcription module.

In the replication and transcription module, several genes related to DNA replication (DNA helicase, DNA primase, resolvase, DNA polymerase, and DNA repair protein), synthesis of DNA precursors (ribonucleotide reductase), and gene regulation (sigma factor and integration host factor) were identified. Additionally, two direct repeats of 41 nucleotides were found in the phiIPLA-RODI genome, between *orf60* and *orf61* (AAAAAGTAC GTATTTAGAAAATAAGGAACTCTCCTATTATA). These sequences share the 27 first nucleotides with a sequence of 28 nucleotides conserved in the *Myoviridae* family of phages infecting *Staphylococcus* (except in phages Romulus, Remus, SA11, phiIBB-SEP1, and Twort). These regions are supposed to be potential binding sites for the replication initiator protein.

A group I intron associated with a VRS endonuclease was detected in the middle of the terminase large subunit gene (*orf68*) in phiIPLA-RODI, while in phiIPLA-C1C, two introns and one intein were identified. The group I intron GIY-YIG homing endonucleases were located interrupting the ribonucleotide reductase large subunit (*orf61*) and DNA polymerase (*orf69*) genes. The intein DOD homing endonuclease is encoded after the recombination protein (*orf73*). Additionally, in phiIPLA-C1C, two intronless ORFs encoding homing endonucleases (GIY-YIG and HNH) were located in intergenic regions after *orf171* and *orf185*, respectively.

Comparative genomics. To perform comparative genomics, genomes of *Myoviridae* phages infecting *Staphylococcus* were colinearized to start at the terminase large subunit. At the nucleotide level, phage phiIPLA-C1C shares a similarity of 80.2% with the only *S. epidermidis*-specific myophage, phiIBB-SEP1 (Table 2), whereas its similarity with the *S. aureus* phages is <55%, suggesting that phiIPLA-C1C might be specific for *S. epidermidis*. Phage phiIPLA-RODI is more closely related to the other phages in the database (identities of over 80%), excluding phage phiIBB-SEP1 and the representative phage Twort, in which case the similarity is <56% (Table 2).

A MAUVE comparison allowed us to determine that all of these phages possess the same general modular structure, including the morphogenesis, replication/transcription, long terminal repeat, and lysis modules. The morphogenesis and replication/transcription modules are conserved among the *Myoviridae* phages infecting *Staphylococcus* (Fig. 2 and 3; see Fig. S2 in the supplemental material). The internal organization in these regions is highly dependent on the presence of homing endonucleases and transposases. Regarding the LTR region, phage phiIPLA-RODI shared homology with all the phages except Twort, phiIPLA-C1C, and phiIBB-SEP1. The phages phiIPLA-C1C and phiIBB-SEP1 possess a specific organization in the LTR region that is not shared with the other phages. The most variable regions at the nucleotide level are located upstream of the LTR region, in which differences regarding the length and gene arrangement are found (see Fig. S2).

Killing of planktonic staphylococcal cultures by phiIPLA-RODI and phiIPLA-C1C. Phages phiIPLA-RODI and phiIPLA-C1C had the same lytic activity on *S. aureus* IPLA16, since no viable bacteria were detected after 8 h of incubation and a considerable decrease of the bacterial population was already achieved after 6 h of treatment (7.9 log units compared to the control). Note that both phages halted growth during the first 4 h, keeping bacterial counts at 10^5 CFU/ml (Fig. 5A). When *S. epidermidis* LO5081 was infected by either phage, no viable counts were de-

TABLE 2 Comparative genomic analysis of *Myoviridae* phages infecting *Staphylococcus*, using Emboss Stretcher

Phage	% similarity	
	phiIPLA-C1C	phiIPLA-RODI
phiIPLA-C1C	100	54.8
phiIPLA-RODI	54.8	100
G1	54.6	83.5
GH15	54.2	84.3
JD007	54.1	83.5
K	53.6	81.1
Twort	53.4	54.5
vB_SauM_Remus	53.6	54.6
vB_SauM_Romulus	52.9	54.2
SA11	54.7	56.2
SA1	44.1	44.7
ISP	54.7	83.8
A5W	54.7	83.2
Sb-1	54.1	79
SA5	54.3	83.1
S25-3	55.1	81.2
S25-4	55.3	80.1
SA012	54.8	81.6
phiIBB-SEP1	80.2	55.8
P4W	55.1	83.6
MSA6	54.9	81.7
Fi200w	55	84.2
676Z	55	84.3
A3R	55.1	82.6
Staph1N	54.7	83.1

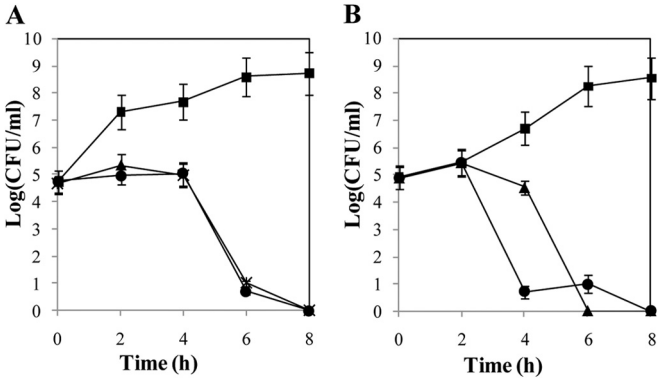

FIG 5 Susceptibilities of *S. aureus* IPLA16 (A) and *S. epidermidis* LO5081 (B) to phages phiIPLA-RODI and phiIPLA-C1C. Cell counts of control cultures (■) and cultures treated with phiIPLA-RODI (▲) or phiIPLA-C1C (●) are represented as log (CFU/ml). Each value corresponds to the mean ± standard deviation for three independent experiments.

tected after 8 h of incubation (Fig. 5B). However, phiIPLA-C1C killed host cells more quickly than phiIPLA-RODI did, and after 4 h of incubation, only 10 CFU/ml viable cells remained. As expected, the number of phages increased in all infected cultures, to about 10^9 PFU/ml (data not shown).

phiIPLA-RODI proved to be more effective than phiIPLA-C1C for removal of mono- and dual-species staphylococcal biofilms. To perform challenge assays against mono- and dual-species biofilms, an *S. aureus* IPLA16-derived strain that is resistant to rifampin (*S. aureus* IPLA16-rif^R) was isolated, with the same phage sensitivity and biofilm formation as its parent (data not shown). *S. aureus* IPLA16-rif^R and *S. epidermidis* LO5081 were grown in both mono- and dual-species biofilms and treated with the phages individually and as a mixture. Numbers of surface-adhered bacteria were successfully reduced after phage treatment (Fig. 6A). In the presence of phiIPLA-RODI, a reduction of 2.43 log units was achieved for *S. aureus* IPLA16-rif^R, with a reduction of 1.89 log units for *S. epidermidis* LO5081. Phage phiIPLA-C1C showed a reduced lytic ability against both staphylococcal biofilms, with reductions in viable counts of 1.84 and 1.16 log units for *S. aureus* IPLA16-rif^R and *S. epidermidis* LO5081, respectively. No significant reduction beyond that recorded for individual phages was observed on biofilms treated with a mixture of phages (Fig. 6A).

Planktonic cells of *S. aureus* IPLA16-rif^R were more sensitive to lysis by phage phiIPLA-RODI (reduction of 4.27 log units) than by phage phiIPLA-C1C (reduction of 0.76 log unit) (Fig. 6A). However, neither individual phage nor the phage mixture was able to kill planktonic *S. epidermidis* LO5081 (ANOVA; $P > 0.05$) (Fig. 6A).

In dual-species biofilms, treatment with phage phiIPLA-RODI showed a reduction in adhered cells of 4.27 log units for *S. aureus* IPLA16-rif^R and of 2.66 log units for *S. epidermidis* LO5081 (Fig. 6B). Treatment of biofilms with phiIPLA-C1C was found to be more effective than that observed in individual biofilms, with a decrease in the adhered cells of 3.23 log units for *S. aureus* IPLA16-rif^R and 2.64 log units for *S. epidermidis* LO5081. Similar to the monospecies biofilm challenge, the mixture of phages did not clearly improve the results obtained by individual phages.

Regarding the planktonic cells, the efficacy of phiIPLA-RODI was higher than that shown by phiIPLA-C1C against both strains forming the dual-species biofilm (Fig. 6B). A reduction of 5.69 log units in *S. aureus* IPLA16-rif^R and of 0.64 log unit in *S. epidermidis* LO5081 was obtained. For phiIPLA-C1C, only a weak reduction in viable counts was detected for *S. aureus* IPLA16-rif^R (Fig. 6B). Treatment with a mixture of phages gave similar results to those obtained using phiIPLA-RODI.

Crystal violet staining was used to confirm the reduction in the total biomass of phage-treated biofilms (Fig. 6C). Overall, removal of biomass by phage treatment in mono- and dual-species biofilms was in accordance with the viable count results (see above). However, in terms of total biomass, the phage treatment turned out to be more effective when a mixture of both phages was applied to both an *S. epidermidis* LO5081 single-species biofilm and the dual-species biofilm (Fig. 6C). Similarly, the treatment with phiIPLA-RODI was more effective than that with phiIPLA-C1C. However, in biofilms formed only by *S. aureus* IPLA16-rif^R, all the treatments were found to have similar detachment abilities.

A phage resistance phenotype has an important fitness cost and is highly unstable. BIMs of *S. aureus* IPLA16 after treatment with phiIPLA-RODI (MOI = 100) and of *S. epidermidis* LO5081 treated with phiIPLA-C1C (MOI = 1,000) emerged at frequencies of $4.05 \times 10^{-7} \pm 2.34 \times 10^{-9}$ and $1.1 \times 10^{-7} \pm 2.08 \times 10^{-9}$, respectively. To test whether resistance implies fitness costs, three phage-resistant colonies of *S. aureus* IPLA16 (*S. aureus* IPLA16-R40, *S. aureus* IPLA16-R53, and *S. aureus* IPLA16-R71) and two phage-resistant colonies of *S. epidermidis* LO5081 (*S. epidermidis* LO5081-R49 and *S. epidermidis* LO5081-R32) were randomly selected for further microbiological characterization (Table 3).

In phage-free liquid cultures, all the BIMs formed aggregates as observed by optical microscopy (see Fig. S3 in the supplemental material). Moreover, the growth rate of BIMs was clearly reduced compared to that of wild-type strains (Table 3). Other parameters indicative of cellular fitness, such as the ability of BIMs to grow in high NaCl concentrations and to form biofilms on polystyrene surfaces, were also determined. *S. aureus* IPLA16-derived BIMs were sensitive to 8% NaCl (Table 3), whereas *S. epidermidis* LO5081-derived BIMs showed resistance to NaCl similar to that of control cultures. Phage-resistant bacteria of both species had a reduced capacity to form biofilms on polystyrene surfaces (up to a 4-fold reduction for *S. aureus* IPLA16 BIMs and up to a 25-fold reduction for *S. epidermidis* LO5081-R33), except for *S. epidermidis* LO5081-R49, which showed values similar to those of the wild-type strain (Table 3).

Regardless of the phage against which BIMs had arisen, they were also resistant to either phiIPLA-RODI or phiIPLA-CIC as well as to phages vB_SauS_phiIPLA88 (44) and vB_SepS_phiIPLA5 (24), two *Siphoviridae* staphylococcal phages (data not shown). Cross-resistance suggested that impaired phage infection may have been due to a lower or nonexistent adsorption of phages. The kinetics of phage binding indicated that adsorption of phiIPLA-RODI and phiIPLA-C1C proceeded to 87 to 90% in 15 min for wild-type strains, while the adsorption rates of BIMs were reduced to 38 to 62% in *S. aureus* and 23% in *S. epidermidis* BIMs (Table 3), indicating that phage infection was prevented by low adsorption of phages to the bacterial surface. Changes in cell surface properties were further confirmed by the significantly less hydrophobic character of the BIMs than of the wild-type strains (Table 3).

To check whether the phage resistance phenotype of BIMs is

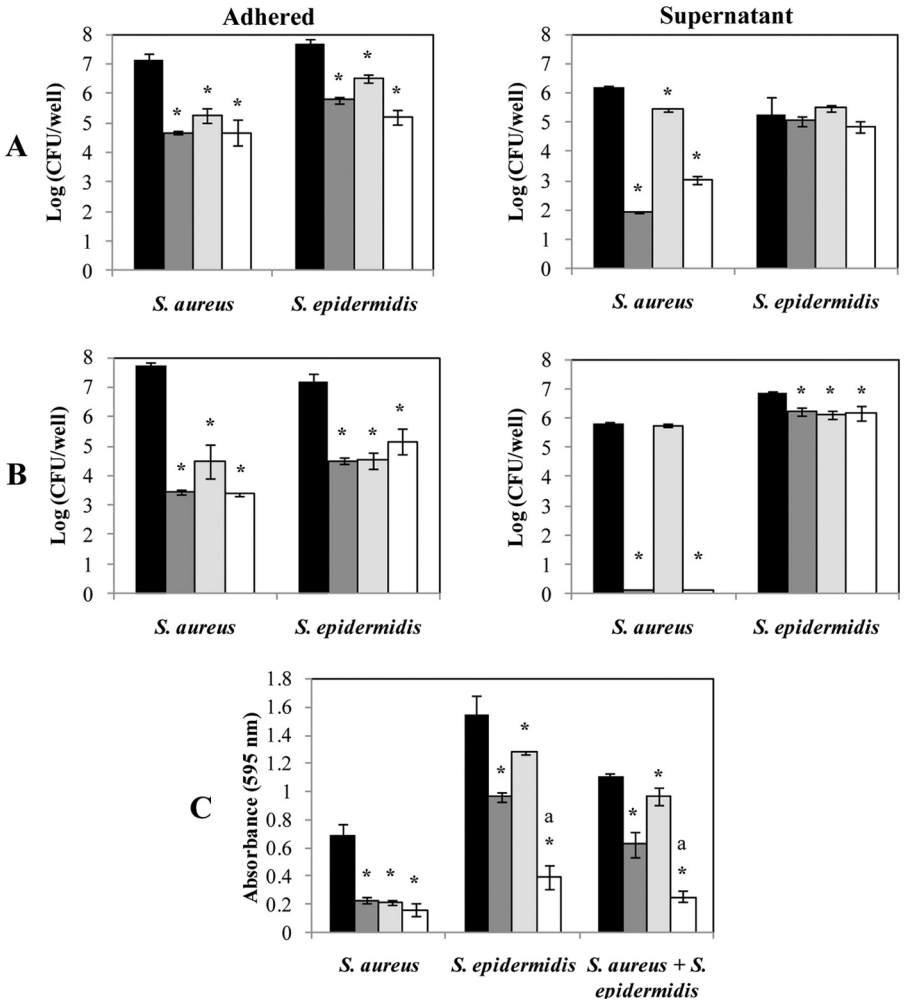

FIG 6 Bacteriophage-mediated removal of 24-h-old *S. aureus* and *S. epidermidis* biofilms. Mono (A)- or dual (B)-species biofilms of *S. aureus* IPLA16-rif^R and *S. epidermidis* LO5081 were treated with phage phiIPLA-RODI (dark gray), phage phiIPLA-C1C (light gray), or a mixture of both phages (white) for 4 h. Data on control biofilms are presented in black. Adhered cell counts and supernatant cell counts are expressed as log (CFU/well). The bacterial detection threshold was 10 log (CFU/ml). (C) Alternatively, the biomass was calculated by crystal violet staining of adhered cells after phage treatment. The absorbance was measured at a wavelength of 595 nm. Means and standard deviations were calculated for three biological replicates. Bars marked with an asterisk are significantly different from the control (ANOVA; $P < 0.05$), and bars marked with "a" indicate significantly different decreases in biomass between the treatment with the mixture of phages and the individual treatment with either phiIPLA-RODI or phiIPLA-C1C (ANOVA; $P < 0.05$).

stable without the selective pressure of phages, BIMs were subcultured for 57 generations, and their sensitivities to phages phiIPLA-RODI and phiIPLA-C1C were tested. *S. aureus* IPLA16-R40, IPLA16-R53, and IPLA16-R71 showed a highly unstable phenotype, and sensitive cultures (a defined transparent halo was observed) were obtained after 27 generations. More variability was observed for *S. epidermidis* LO5081 BIMs, as *S. epidermidis* LO5081-R49 reverted to the sensitive phenotype after 17 generations, while *S. epidermidis* LO5081-R33 lost phage resistance only after 57 generations (Table 3). Recovery of phage sensitivity was linked to the reestablishment of sensitivity to either phiIPLA-RODI or phiIPLA-C1C and the two *Siphoviridae* phages. Moreover, the original growth rate was also restored (data not shown).

DISCUSSION

Within the bacteriophage therapy context, we have characterized two new lytic phages, phiIPLA-RODI and phiIPLA-C1C, which show the typical wide host range of polyvalent phages, such as phage K and phi812 (45, 46), in contrast to other monovalent myophages, such as Stau2, Romulus, and Remus (28, 47), whose host range is limited to *S. aureus* strains, and phage phiIBB-SEP1, infecting only *S. epidermidis* strains (48).

From the perspective of feasibility for therapeutic application, we determined that the stabilities of phages phiIPLA-RODI and phiIPLA-C1C at various pHs and temperatures were very similar to those described for related phages, such as MSA6 (49) and Romulus and Remus (28), and therefore that these phages are suitable for design of different pharmaceutical formulations by lyophilization (50), spray drying (51), and aerosolization (52). Bioinformatic analysis of the phiIPLA-RODI and phiIPLA-C1C genomes showed the typical characteristics of the "Twort-like viruses" (*Spounavirinae* subfamily): strictly virulent, with large genomes (127 to 140 kb) containing LTRs, genes grouped into modules that are not clearly separated, a few genes encoding tRNAs,

TABLE 3 Fitness of *S. aureus* IPLA16 and *S. epidermidis* LO5081, and their BIMs, against phages phiIPLA-RODI and phiIPLA-C1C, respectively[a]

Strain	Growth rate (μ) (h^{-1})	LD_{50} of NaCl (%)	Biofilm formation (OD_{595})	% phage adsorption in 15 min	Adsorption rate constant (k) (ml/min)	Hydrophobicity (% adhesion to hexadecane)	Generation after which reversion occurred
S. aureus IPLA16	0.76 ± 0.02	8.14 ± 0.42	1.13 ± 0.06	87.67 ± 3.74	$8.9 \times 10^{-11} \pm 7.5 \times 10^{-12}$	85.62 ± 5.47	
S. aureus IPLA16-R40	0.56 ± 0.02*	6.12 ± 0.33*	0.31 ± 0.01*	62.66 ± 2.09*	$3.1 \times 10^{-10} \pm 7.1 \times 10^{-11}$*	44.47 ± 7.67*	27
S. aureus IPLA16-R53	0.59 ± 0.04*	4.80 ± 0.23*	0.28 ± 0.02*	38.33 ± 6.21*	$6.5 \times 10^{-10} \pm 1.7 \times 10^{-11}$*	32.13 ± 8.37*	27
S. aureus IPLA16-R71	0.49 ± 0.03*	2.82 ± 0.34*	0.41 ± 0.02*	39.66 ± 3.25*	$6.2 \times 10^{-10} \pm 1.2 \times 10^{-11}$*	34.77 ± 8.17*	27
S. epidermidis LO5081	0.74 ± 0.03	8.23 ± 0.74	9.81 ± 0.38	90.60 ± 8.19	$6.5 \times 10^{-11} \pm 2.3 \times 10^{-12}$	95.43 ± 2.06	
S. epidermidis LO5081-R32	0.58 ± 0.02*	8.15 ± 0.25	0.39 ± 0.06*	17.60 ± 7.23*	$6.9 \times 10^{-10} \pm 1.3 \times 10^{-10}$*	33.78 ± 6.65*	57
S. epidermidis LO5081-R49	0.52 ± 0.06*	8.13 ± 0.08	8.99 ± 0.47	23.00 ± 5.69*	$9.9 \times 10^{-10} \pm 1.7 \times 10^{-10}$*	77.05 ± 11.31*	17

[a] Values represent the means ± standard deviations for three biological replicates. The presence of an asterisk indicates those values that are significantly different from those of the wild-type strain (ANOVA; $P < 0.05$).

and the presence of group I introns (42). The genome of phage phiIPLA-C1C differs from those of the above-mentioned phages in the lack of genes encoding tRNAs, a peculiarity already observed in the *S. epidermidis* phage phiIBB-SEP1 (48). In addition, the nucleotide genome sequence of phiIPLA-RODI showed a lack of restriction sites for the endonucleases Sau3AI, BamHI, and BglII, but these are present in the phiIPLA-C1C genome. This appears to be a general strategy among *S. aureus* bacteriophages, such as Twort, K, G1, Sb-1, and MSA6, to avoid restriction by host bacteria (49, 53).

Both phages encode homing endonucleases, found within group I introns, intergenic regions, or inteins, in accordance with previous results reported for other myophages, such as T4, where 11% of the ORFs correspond to homing endonucleases (54). In T4-related phages, most of the homing endonucleases belong to the GIY-YIG and HNH families, with multiple functions, such as recombination and binding to and repair of DNA (54). Homing endonucleases encoded by phiIPLA-C1C were not identified in other phage genomes, consistent with the idea that these proteins are a recent evolutionary acquisition that may have an influence on gene arrangement and function and that, in addition, they may promote their own spread between phages (54).

Once the phages were morphologically and genetically characterized, we proceeded to study their lytic activity against staphylococcal bacteria in both planktonic cultures and preformed biofilms. The results of biofilm removal assays confirmed that phage infection in planktonic cell cultures is more efficient than that in biofilms. Overall, *S. aureus* IPLA16 biofilms were well infected by both phages, while *S. epidermidis* LO5081 biofilms were found to be more resistant to phage predation. A likely explanation is the higher content of extracellular matrix formed by *S. epidermidis* LO5081 than by *S. aureus* IPLA16, which may hinder the access of phages to bacteria. Some phages encode polysaccharide depolymerase proteins which degrade the extracellular matrix of biofilms, facilitating the access of phages to target bacteria (20). However, no genes encoding proteins with these catalytic domains were detected in either the phiIPLA-RODI or phiIPLA-C1C genome. After biofilm treatment, it was also quite surprising that detached cells were not killed by phages, except those released from *S. aureus* IPLA16 biofilms treated with phiIPLA-RODI. These data suggest that cells released from inside a biofilm are not susceptible to phage infection due to their unique physiological state (22). The biomass reductions of *S. aureus* IPLA16 biofilms by these phages were similar (67% for phage phiIPLA-RODI and 69% for phage phiIPLA-C1C) to those obtained with phages ISP, Romulus, and Remus (28). The complete eradication of biofilms by phages has not been described in the literature to date. However, prevention of biofilm formation has been achieved for *S. aureus* Xen29 biofilms, using a combination of phage K and modified derivatives (21). In addition, *S. aureus* biofilms could be eradicated efficiently with a combination of phage SAP-26 and rifampin (55).

Phage control of dual-species biofilms was investigated using *S. aureus* and *S. epidermidis* as a proof of concept to evaluate whether the mixture of both phages could be more effective than each individual phage. Our results provide evidence that phages can reduce the cell numbers of both species, but the application of a phage mixture against each of the hosts was not always more effective than the use of only one phage. Indeed, the addition of the single phage phiIPLA-RODI resulted in a reduction similar to that achieved by the mixture of phages. The low efficacy of phiIPLA-C1C may be due to the lower burst size of this phage than that of phiIPLA-RODI. Overall, these results are in agreement with those obtained by other authors (56, 57), who reported reductions of about 3 to 4 log units in viable cells from mixed biofilms treated with phages. Mixed-species biofilms are complex communities in which the physiological state of cells and the availability of phage receptors play important roles in the behavior of phages (58). These features may be altered drastically by competition with other bacterial species. In mixed cultures of *Escherichia coli* and *Salmonella*, phages against *E. coli* were more effective at removing this species than in monocultures of *E. coli*. It seems that for some bacteria, the competition with other bacterial species may enhance the effectiveness of phages, because phage bacterial resistance can decrease the competitive ability of bacteria (59). Similar

data were observed in our staphylococcal biofilms, in which treatment with phages turned to be more effective in dual-species biofilms than in monospecies biofilms.

Phage resistance is often a major concern in the therapeutic application of phages, as it may compromise the efficacy of the treatment (60). In this regard, the frequencies of bacteria acquiring resistance to phages phiIPLA-RODI and phiIPLA-C1C were determined to be low, and most important, the global fitness of staphylococcal BIMs was clearly affected. This reduced fitness of phage-resistant bacteria was also observed for different species, such as *Vibrio cholerae* (61) and *Pseudomonas aeruginosa* (62). We have not determined the molecular basis of the phage resistance mechanisms in the BIMs. However, it is known that wall teichoic acid (WTA) serves as a receptor for several staphylococcal siphoviruses and myoviruses (63). Therefore, a lack of WTA in *S. aureus* and *S. epidermidis* BIMs might explain the resistance of these strains to phages belonging to the *Siphoviridae* and *Myoviridae* families. In addition, phiIPLA-RODI and phiIPLA-C1C BIMs were shown to be more sensitive to high temperatures, showed higher degrees of cell aggregation, and had a reduced capacity to form biofilms, as previously observed in *S. aureus* WTA-deficient mutants (64). However, we cannot disregard the presence of a capsular polysaccharide in staphylococcal BIMs, which may modify the bacterial surface properties and prevent phage adsorption to the cell (65).

The data presented in this study support the potential of the lytic bacteriophages phiIPLA-RODI and phiIPLA-C1C to be used in phage therapy. Their characterization indicates a wide host range, an adequate stability in various environmental conditions, a lack of virulence factors, the capability to remove biofilms, and a low frequency of BIMs.

ACKNOWLEDGMENTS

This research study was supported by grants AGL2012-40194-C02-01 (Ministry of Science and Innovation, Spain) and GRUPIN14-139 (Program of Science, Technology and Innovation 2013–2017, Principado de Asturias, Spain) and by the bacteriophage network FAGOMA. D.G. is a fellow of the Ministry of Science and Innovation, Spain. P.G., B.M., and A.R. are members of the FWO Vlaanderen-funded Phagebiotics research community (WO.016.14). D.V. holds a Ph.D. scholarship from the IWT Vlaanderen.

We thank R. Calvo (IPLA-CSIC) for technical assistance.

REFERENCES

1. **Otto M.** 2013. Staphylococcal infections: mechanisms of biofilm maturation and detachment as critical determinants of pathogenicity. Annu Rev Med **64:**175–188. http://dx.doi.org/10.1146/annurev-med-042711-140023.
2. **Savage VJ, Chopra I, O'Neill AJ.** 2013. *Staphylococcus aureus* biofilms promote horizontal transfer of antibiotic resistance. Antimicrob Agents Chemother **57:**1968–1970. http://dx.doi.org/10.1128/AAC.02008-12.
3. **Rogers KL, Fey PD, Rupp ME.** 2009. Coagulase-negative staphylococcal infections. Infect Dis Clin North Am **23:**73–98. http://dx.doi.org/10.1016/j.idc.2008.10.001.
4. **Hell E, Giske CG, Hultenby K, Danielsson KG, Marchini G.** 2013. Attachment and biofilm forming capabilities of *Staphylococcus epidermidis* strains isolated from preterm infants. Curr Microbiol **67:**712–717. http://dx.doi.org/10.1007/s00284-013-0425-3.
5. **Otto M.** 2009. *Staphylococcus epidermidis*—the 'accidental' pathogen. Nat Rev Microbiol **7:**555–567. http://dx.doi.org/10.1038/nrmicro2182.
6. **Hellmark B, Berglund C, Nilsdotter-Augustinsson A, Unemo M, Soderquist B.** 2013. Staphylococcal cassette chromosome *mec* (SCC*mec*) and arginine catabolic mobile element (ACME) in *Staphylococcus epidermidis* isolated from prosthetic joint infections. Eur J Clin Microbiol Infect Dis **32:**691–697. http://dx.doi.org/10.1007/s10096-012-1796-2.
7. **Periasamy S, Joo HS, Duong AC, Bach TH, Tan VY, Chatterjee SS, Cheung GY, Otto M.** 2012. How *Staphylococcus aureus* biofilms develop their characteristic structure. Proc Natl Acad Sci U S A **109:**1281–1286. http://dx.doi.org/10.1073/pnas.1115006109.
8. **David MZ, Daum RS.** 2010. Community-associated methicillin-resistant *Staphylococcus aureus*: epidemiology and clinical consequences of an emerging epidemic. Clin Microbiol Rev **23:**616–687. http://dx.doi.org/10.1128/CMR.00081-09.
9. **Fessler AT, Kadlec K, Hassel M, Hauschild T, Eidam C, Ehricht R, Monecke S, Schwarz S.** 2011. Characterization of methicillin-resistant *Staphylococcus aureus* isolates from food and food products of poultry origin in Germany. Appl Environ Microbiol **77:**7151–7157. http://dx.doi.org/10.1128/AEM.00561-11.
10. **Price LB, Stegger M, Hasman H, Aziz M, Larsen J, Andersen PS, Pearson T, Waters AE, Foster JT, Schupp J, Gillece J, Driebe E, Liu CM, Springer B, Zdovc I, Battisti A, Franco A, Zmudzki J, Schwarz S, Butaye P, Jouy E, Pomba C, Porrero MC, Ruimy R, Smith TC, Robinson DA, Weese JS, Arriola CS, Yu F, Laurent F, Keim P, Skov R, Aarestrup FM.** 2012. *Staphylococcus aureus* CC398: host adaptation and emergence of methicillin resistance in livestock. mBio **3:**e00305-11. http://dx.doi.org/10.1128/mBio.00305-11.
11. **Kutateladze M, Adamia R.** 2010. Bacteriophages as potential new therapeutics to replace or supplement antibiotics. Trends Biotechnol **28:**591–595. http://dx.doi.org/10.1016/j.tibtech.2010.08.001.
12. **Miedzybrodzki R, Borysowski J, Weber-Dabrowska B, Fortuna W, Letkiewicz S, Szufnarowski K, Pawelczyk Z, Rogoz P, Klak M, Wojtasik E, Gorski A.** 2012. Clinical aspects of phage therapy. Adv Virus Res **83:**73–121. http://dx.doi.org/10.1016/B978-0-12-394438-2.00003-7.
13. **Leszczyński P, Weber-Dabrowska B, Kohutnicka M, Luczak M, Górecki A, Górski A.** 2006. Successful eradication of methicillin-resistant *Staphylococcus aureus* (MRSA) intestinal carrier status in a healthcare worker—case report. Folia Microbiol (Praha) **51:**236–238. http://dx.doi.org/10.1007/BF02932128.
14. **Takemura-Uchiyama I, Uchiyama J, Osanai M, Morimoto N, Asagiri T, Ujihara T, Daibata M, Sugiura T, Matsuzaki S.** 2014. Experimental phage therapy against lethal lung-derived septicemia caused by *Staphylococcus aureus* in mice. Microbes Infect **16:**512–517. http://dx.doi.org/10.1016/j.micinf.2014.02.011.
15. **Takemura-Uchiyama I, Uchiyama J, Kato S, Inoue T, Ujihara T, Ohara N, Daibata M, Matsuzaki S.** 2013. Evaluating efficacy of bacteriophage therapy against *Staphylococcus aureus* infections using a silkworm larval infection model. FEMS Microbiol Lett **347:**52–60. http://dx.doi.org/10.1111/1574-6968.12220.
16. **Drilling A, Morales S, Jardeleza C, Vreugde S, Speck P, Wormald PJ.** 2014. Bacteriophage reduces biofilm of *Staphylococcus aureus* ex vivo isolates from chronic rhinosinusitis patients. Am J Rhinol Allergy **28:**3–11. http://dx.doi.org/10.2500/ajra.2014.28.4001.
17. **Mendes JJ, Leandro C, Corte-Real S, Barbosa R, Cavaco-Silva P, Melo-Cristino J, Gorski A, Garcia M.** 2013. Wound healing potential of topical bacteriophage therapy on diabetic cutaneous wounds. Wound Repair Regen **21:**595–603. http://dx.doi.org/10.1111/wrr.12056.
18. **Chhibber S, Kaur T, Sandeep K.** 2013. Co-therapy using lytic bacteriophage and linezolid: effective treatment in eliminating methicillin resistant *Staphylococcus aureus* (MRSA) from diabetic foot infections. PLoS One **8:**e56022. http://dx.doi.org/10.1371/journal.pone.0056022.
19. **Seth AK, Geringer MR, Nguyen KT, Agnew SP, Dumanian Z, Galiano RD, Leung KP, Mustoe TA, Hong SJ.** 2013. Bacteriophage therapy for *Staphylococcus aureus* biofilm-infected wounds: a new approach to chronic wound care. Plast Reconstr Surg **131:**225–234. http://dx.doi.org/10.1097/PRS.0b013e31827e47cd.
20. **Gutierrez D, Martinez B, Rodriguez A, Garcia P.** 2012. Genomic characterization of two *Staphylococcus epidermidis* bacteriophages with antibiofilm potential. BMC Genomics **13:**228. http://dx.doi.org/10.1186/1471-2164-13-228.
21. **Kelly D, McAuliffe O, Ross RP, Coffey A.** 2012. Prevention of *Staphylococcus aureus* biofilm formation and reduction in established biofilm density using a combination of phage K and modified derivatives. Lett Appl Microbiol **54:**286–291. http://dx.doi.org/10.1111/j.1472-765X.2012.03205.x.
22. **Cerca N, Oliveira R, Azeredo J.** 2007. Susceptibility of *Staphylococcus epidermidis* planktonic cells and biofilms to the lytic action of *Staphylococcus* bacteriophage K. Lett Appl Microbiol **45:**313–317. http://dx.doi.org/10.1111/j.1472-765X.2007.02190.x.

23. **Kropinski AM, Prangishvili D, Lavigne R.** 2009. Position paper: the creation of a rational scheme for the nomenclature of viruses of *Bacteria* and *Archaea*. Environ Microbiol **11:**2775–2777. http://dx.doi.org/10.1111/j.1462-2920.2009.01970.x.
24. **Gutierrez D, Martinez B, Rodriguez A, Garcia P.** 2010. Isolation and characterization of bacteriophages infecting *Staphylococcus epidermidis*. Curr Microbiol **61:**601–608. http://dx.doi.org/10.1007/s00284-010-9659-5.
25. **Gutierrez D, Ruas-Madiedo P, Martinez B, Rodriguez A, Garcia P.** 2014. Effective removal of staphylococcal biofilms by the endolysin LysH5. PLoS One **9:**e107307. http://dx.doi.org/10.1371/journal.pone.0107307.
26. **Bellon-Fontaine MN, Rault J, Van Oss CJ.** 1996. Microbial adhesion to solvents: a novel method to determine the electron-donor/electron-acceptor or Lewis acid-base properties of microbial cells. Colloids Surf B Biointerfaces **7:**47–53. http://dx.doi.org/10.1016/0927-7765(96)01272-6.
27. **Campelo AB, Gaspar P, Roces C, Rodriguez A, Kok J, Kuipers OP, Neves AR, Martinez B.** 2011. The Lcn972 bacteriocin-encoding plasmid pBL1 impairs cellobiose metabolism in *Lactococcus lactis*. Appl Environ Microbiol **77:**7576–7585. http://dx.doi.org/10.1128/AEM.06107-11.
28. **Vandersteegen K, Kropinski AM, Nash JH, Noben JP, Hermans K, Lavigne R.** 2013. Romulus and Remus, two phage isolates representing a distinct clade within the *Twortlikevirus* genus, display suitable properties for phage therapy applications. J Virol **87:**3237–3247. http://dx.doi.org/10.1128/JVI.02763-12.
29. **Garcia P, Rodriguez I, Suarez JE.** 2004. A −1 ribosomal frameshift in the transcript that encodes the major head protein of bacteriophage A2 mediates biosynthesis of a second essential component of the capsid. J Bacteriol **186:**1714–1719. http://dx.doi.org/10.1128/JB.186.6.1714-1719.2004.
30. **Overbeek R, Olson R, Pusch GD, Olsen GJ, Davis JJ, Disz T, Edwards RA, Gerdes S, Parrello B, Shukla M, Vonstein V, Wattam AR, Xia F, Stevens R.** 2014. The SEED and the rapid annotation of microbial genomes using subsystems technology (RAST). Nucleic Acids Res **42:**D206–D214. http://dx.doi.org/10.1093/nar/gkt1226.
31. **Altschul SF, Gish W, Miller W, Myers EW, Lipman DJ.** 1990. Basic local alignment search tool. J Mol Biol **215:**403–410. http://dx.doi.org/10.1016/S0022-2836(05)80360-2.
32. **Zdobnov EM, Apweiler R.** 2001. InterProScan—an integration platform for the signature-recognition methods in InterPro. Bioinformatics **17:**847–848. http://dx.doi.org/10.1093/bioinformatics/17.9.847.
33. **Bailey TL, Boden M, Buske FA, Frith M, Grant CE, Clementi L, Ren J, Li WW, Noble WS.** 2009. MEME SUITE: tools for motif discovery and searching. Nucleic Acids Res **37:**W202–W208. http://dx.doi.org/10.1093/nar/gkp335.
34. **Naville M, Ghuillot-Gaudeffroy A, Marchais A, Gautheret D.** 2011. ARNold: a web tool for the prediction of Rho-independent transcription terminators. RNA Biol **8:**11–13. http://dx.doi.org/10.4161/rna.8.1.13346.
35. **Ermolaeva MD, Khalak HG, White O, Smith HO, Salzberg SL.** 2000. Prediction of transcription terminators in bacterial genomes. J Mol Biol **301:**27–33. http://dx.doi.org/10.1006/jmbi.2000.3836.
36. **Schattner P, Brooks AN, Lowe TM.** 2005. The tRNAscan-SE, snoscan and snoGPS web servers for the detection of tRNAs and snoRNAs. Nucleic Acids Res **33:**W686–W689. http://dx.doi.org/10.1093/nar/gki366.
37. **Laslett D, Canback B.** 2004. ARAGORN, a program to detect tRNA genes and tmRNA genes in nucleotide sequences. Nucleic Acids Res **32:**11–16. http://dx.doi.org/10.1093/nar/gkh152.
38. **Myers EW, Miller W.** 1988. Optimal alignments in linear space. Comput Appl Biosci **4:**11–17.
39. **Darling AE, Mau B, Perna NT.** 2010. progressiveMauve: multiple genome alignment with gene gain, loss and rearrangement. PLoS One **5:**e11147. http://dx.doi.org/10.1371/journal.pone.0011147.
40. **Grant JR, Stothard P.** 2008. The CGView server: a comparative genomics tool for circular genomes. Nucleic Acids Res **36:**W181–W184. http://dx.doi.org/10.1093/nar/gkn179.
41. **Klumpp J, Lavigne R, Loessner MJ, Ackermann HW.** 2010. The SPO1-related bacteriophages. Arch Virol **155:**1547–1561. http://dx.doi.org/10.1007/s00705-010-0783-0.
42. **Lobocka M, Hejnowicz MS, Dabrowski K, Gozdek A, Kosakowski J, Witkowska M, Ulatowska MI, Weber-Dabrowska B, Kwiatek M, Parasion S, Gawor J, Kosowska H, Glowacka A.** 2012. Genomics of staphylococcal Twort-like phages—potential therapeutics of the post-antibiotic era. Adv Virus Res **83:**143–216. http://dx.doi.org/10.1016/B978-0-12-394438-2.00005-0.
43. **Stewart CR, Yip TK, Myles B, Laughlin L.** 2009. Roles of genes 38, 39, and 40 in shutoff of host biosyntheses during infection of *Bacillus subtilis* by bacteriophage SPO1. Virology **392:**271–274. http://dx.doi.org/10.1016/j.virol.2009.06.046.
44. **Garcia P, Martinez B, Obeso JM, Lavigne R, Lurz R, Rodriguez A.** 2009. Functional genomic analysis of two *Staphylococcus aureus* phages isolated from the dairy environment. Appl Environ Microbiol **75:**7663–7673. http://dx.doi.org/10.1128/AEM.01864-09.
45. **O'Flaherty S, Ross RP, Meaney W, Fitzgerald GF, Elbreki MF, Coffey A.** 2005. Potential of the polyvalent anti-*Staphylococcus* bacteriophage K for control of antibiotic-resistant staphylococci from hospitals. Appl Environ Microbiol **71:**1836–1842. http://dx.doi.org/10.1128/AEM.71.4.1836-1842.2005.
46. **El Haddad L, Ben Abdallah N, Plante PL, Dumaresq J, Katsarava R, Labrie S, Corbeil J, St-Gelais D, Moineau S.** 2014. Improving the safety of *Staphylococcus aureus* polyvalent phages by their production on a *Staphylococcus xylosus* strain. PLoS One **9:**e102600. http://dx.doi.org/10.1371/journal.pone.0102600.
47. **Hsieh SE, Lo HH, Chen ST, Lee MC, Tseng YH.** 2011. Wide host range and strong lytic activity of *Staphylococcus aureus* lytic phage Stau2. Appl Environ Microbiol **77:**756–761. http://dx.doi.org/10.1128/AEM.01848-10.
48. **Melo LD, Sillankorva S, Ackermann HW, Kropinski AM, Azeredo J, Cerca N.** 2014. Isolation and characterization of a new *Staphylococcus epidermidis* broad-spectrum bacteriophage. J Gen Virol **95:**506–515. http://dx.doi.org/10.1099/vir.0.060590-0.
49. **Kwiatek M, Parasion S, Mizak L, Gryko R, Bartoszcze M, Kocik J.** 2012. Characterization of a bacteriophage, isolated from a cow with mastitis, that is lytic against *Staphylococcus aureus* strains. Arch Virol **157:**225–234. http://dx.doi.org/10.1007/s00705-011-1160-3.
50. **Merabishvili M, Vervaet C, Pirnay JP, De Vos D, Verbeken G, Mast J, Chanishvili N, Vaneechoutte M.** 2013. Stability of *Staphylococcus aureus* phage ISP after freeze-drying (lyophilization). PLoS One **8:**e68797. http://dx.doi.org/10.1371/journal.pone.0068797.
51. **Vandenheuvel D, Singh A, Vandersteegen K, Klumpp J, Lavigne R, Van den Mooter G.** 2013. Feasibility of spray drying bacteriophages into respirable powders to combat pulmonary bacterial infections. Eur J Pharm Biopharm **84:**578–582. http://dx.doi.org/10.1016/j.ejpb.2012.12.022.
52. **Turgeon N, Toulouse MJ, Martel B, Moineau S, Duchaine C.** 2014. Comparison of five bacteriophages as models for viral aerosol studies. Appl Environ Microbiol **80:**4242–4250. http://dx.doi.org/10.1128/AEM.00767-14.
53. **Andriashvili IA, Kvachadze LI, Bashakidze RP, Adamiia R, Chanishvili TG.** 1986. Molecular mechanism of phage DNA protection from the restriction endonucleases of *Staphylococcus aureus* cells. Mol Gen Mikrobiol Virusol **1986:**43–45.
54. **Edgell DR, Gibb EA, Belfort M.** 2010. Mobile DNA elements in T4 and related phages. Virol J **7:**290. http://dx.doi.org/10.1186/1743-422X-7-290.
55. **Rahman M, Kim S, Kim SM, Seol SY, Kim J.** 2011. Characterization of induced *Staphylococcus aureus* bacteriophage SAP-26 and its anti-biofilm activity with rifampicin. Biofouling **27:**1087–1093. http://dx.doi.org/10.1080/08927014.2011.631169.
56. **Carson L, Gorman SP, Gilmore BF.** 2010. The use of lytic bacteriophages in the prevention and eradication of biofilms of *Proteus mirabilis* and *Escherichia coli*. FEMS Immunol Med Microbiol **59:**447–455. http://dx.doi.org/10.1111/j.1574-695X.2010.00696.x.
57. **Sillankorva S, Neubauer P, Azeredo J.** 2010. Phage control of dual species biofilms of *Pseudomonas fluorescens* and *Staphylococcus lentus*. Biofouling **26:**567–575. http://dx.doi.org/10.1080/08927014.2010.494251.
58. **Sutherland IW, Hughes KA, Skillman LC, Tait K.** 2004. The interaction of phage and biofilms. FEMS Microbiol Lett **232:**1–6. http://dx.doi.org/10.1016/S0378-1097(04)00041-2.
59. **Harcombe WR, Bull JJ.** 2005. Impact of phages on two-species bacterial communities. Appl Environ Microbiol **71:**5254–5259. http://dx.doi.org/10.1128/AEM.71.9.5254-5259.2005.
60. **Ormala AM, Jalasvuori M.** 2013. Phage therapy: should bacterial resistance to phages be a concern, even in the long run? Bacteriophage **3:**e24219. http://dx.doi.org/10.4161/bact.24219.
61. **Zahid MS, Udden SM, Faruque AS, Calderwood SB, Mekalanos JJ, Faruque SM.** 2008. Effect of phage on the infectivity of *Vibrio cholerae* and emergence of genetic variants. Infect Immun **76:**5266–5273. http://dx.doi.org/10.1128/IAI.00578-08.

62. **Hall AR, De Vos D, Friman VP, Pirnay JP, Buckling A.** 2012. Effects of sequential and simultaneous applications of bacteriophages on populations of *Pseudomonas aeruginosa in vitro* and in wax moth larvae. Appl Environ Microbiol **78:**5646–5652. http://dx.doi.org/10.1128/AEM.00757-12.
63. **Xia G, Corrigan RM, Winstel V, Goerke C, Grundling A, Peschel A.** 2011. Wall teichoic acid-dependent adsorption of staphylococcal siphovirus and myovirus. J Bacteriol **193:**4006–4009. http://dx.doi.org/10.1128/JB.01412-10.
64. **Vergara-Irigaray M, Maira-Litran T, Merino N, Pier GB, Penades JR, Lasa I.** 2008. Wall teichoic acids are dispensable for anchoring the PNAG exopolysaccharide to the *Staphylococcus aureus* cell surface. Microbiology **154:**865–877. http://dx.doi.org/10.1099/mic.0.2007/013292-0.
65. **Labrie SJ, Samson JE, Moineau S.** 2010. Bacteriophage resistance mechanisms. Nat Rev Microbiol **8:**317–327. http://dx.doi.org/10.1038/nrmicro2315.
66. **Gutierrez D, Delgado S, Vazquez-Sanchez D, Martinez B, Cabo ML, Rodriguez A, Herrera JJ, Garcia P.** 2012. Incidence of *Staphylococcus aureus* and analysis of associated bacterial communities on food industry surfaces. Appl Environ Microbiol **78:**8547–8554. http://dx.doi.org/10.1128/AEM.02045-12.
67. **Valle J, Toledo-Arana A, Berasain C, Ghigo JM, Amorena B, Penades JR, Lasa I.** 2003. SarA and not σ^B is essential for biofilm development by *Staphylococcus aureus*. Mol Microbiol **48:**1075–1087. http://dx.doi.org/10.1046/j.1365-2958.2003.03493.x.
68. **Cucarella C, Solano C, Valle J, Amorena B, Lasa I, Penades JR.** 2001. Bap, a *Staphylococcus aureus* surface protein involved in biofilm formation. J Bacteriol **183:**2888–2896. http://dx.doi.org/10.1128/JB.183.9.2888-2896.2001.
69. **Delgado S, Arroyo R, Jimenez E, Marin ML, del Campo R, Fernandez L, Rodriguez JM.** 2009. *Staphylococcus epidermidis* strains isolated from breast milk of women suffering infectious mastitis: potential virulence traits and resistance to antibiotics. BMC Microbiol **9:**82. http://dx.doi.org/10.1186/1471-2180-9-82.
70. **Martin V, Maldonado-Barragan A, Moles L, Rodriguez-Banos M, Campo RD, Fernandez L, Rodriguez JM, Jimenez E.** 2012. Sharing of bacterial strains between breast milk and infant feces. J Hum Lact **28:**36–44. http://dx.doi.org/10.1177/0890334411424729.